Ab initio calculation of ligand field multiplet parameters for transition metal L-edge spectra

Peter Krüger

Graduate School of Engineering and Molecular Chirality Research Center, Chiba University, Chiba 263-8522, Japan

A B S T R A C T

A simple method for non-empirical ligand field multiplet calculations for transition metal L-edge spectra is presented. Ligand field splittings and anisotropic scaling factors for Coulomb integrals are obtained from density functional theory. The method is applied to transition metal monoxide solids and nickel and cobalt phthalocyanines molecules and good agreement with experiment is obtained.

1. Introduction

X-ray absorption spectroscopy at the transition metal $L_{2,3}$-edges probes the $2p$ to $3d$ transitions and is a precious source of information about valence, magnetism and bonding of the metal site in a compound or molecule (de Groot and Kotani, 2008). The standard calculation method for L-edge spectra is ligand field multiplet (LFM) theory (Yamaguchi et al., 1982; van der Laan et al., 1988; Thole and van der Laan, 1988). LFM theory is based on a single ion model, where Coulomb and spin-orbit interactions are computed ab initio from Hartree-Fock wave functions. The perturbation of the free ion electronic structure by the ligands is described by introducing a symmetry-dependent level splitting of the $3d$-orbitals and by rescaling the Coulomb (Slater-Condon) integrals by a constant reduction factor κ. This simple treatment of all extra-atomic effects has proven astonishingly successful, especially in high-symmetry ionic compounds (de Groot et al., 1990). The major drawback is that it relies on empirical parameters. The number of parameters required to describe the splitting of the 3d-level depends on the point group symmetry. This number is one for cubic (Dq), three for tetrahedral symmetry (Dq, Ds, Dt) but raises to 15 in absence of any point symmetry (C_1). In systems relevant for nanoscience, biology and catalys, the point symmetry at the transition metal ion site is often low and thus the number of ligand field parameters is large. Then, parameter fitting becomes cumbersome and the theory lacks any predictive power.

Here we introduce a simple method for computing the parameters of LFM model from density functional theory (DFT). The orbital dependence of Coulomb integral reduction is taken into account for the first time in LFM calculations. We apply the method to L-edge spectra of transition metal monoxides as well as nickel and cobalt phthalocyanine molecules, and obtain good agreement with experiment in all cases.

2. Theory

We wish to calculate the absorption spectrum from the $L_{2,3}$ edges of a transition metal site of an extended system, either molecule or solid, using the LFM model. In order to obtain the LFM parameters, we first determine the valence electronic structure of the extended system using DFT from which we obtain the single-particle eigenvalues ε_k and eigenstates ψ_k. These molecular or band orbitals ψ_k are projected on $3d$-orbital basis states ϕ_m centered on the metal site, where m denotes one of the five d-orbitals symmetries, usually taken as real spherical harmonics. Ideally, the $3d$ orbital basis corresponds to the free ion calculation from which the multiplet (Coulomb-integrals and spin-orbit) parameters are obtained. In practice, other local orbital projection schemes can be expected to give very similar results. Here we use the projector-augmented wave method as implemented in VASP (Kresse and Furthmüller, 1996) with projection in atomic spheres. The atomic sphere radii are chosen as the Wigner-Seitz radii of the elemental metals. The projection yields the $3d$-wave amplitudes

$$C_{mk} = \langle \phi_m | \psi_k \rangle \tag{1}$$

We define an energy range $I = (E_1, E_2)$ which covers the eigenvalues ε_k whose eigenfunctions ψ_k have dominant transition metal $3d$-character. For transition metal oxides, for example, the interval I should cover the antibonding $3d$-like bands. The definition of the energy intervall I is the only part of the procedure which requires a choice by the user. We define orbital reduction factors α_m as

$$|\alpha_m|^2 = \sum_k{}' |C_{mk}|^2 \tag{2}$$

where ' indicates that the sum runs only over eigenstates with $\varepsilon_k \in I$. We choose the phase of α_m as real positive for convenience. The ligand field splittings are obtained from the effective $3d$ levels ε_m defined as

$$\varepsilon_m = |\alpha_m|^{-2} \sum_k {}' \varepsilon_k |C_{mk}|^2 \tag{3}$$

Thus the levels ε_m are taken as a sum over molecular levels or band energies, weighted by the $3d$-m partial density of states (DOS). The matrix elements of the electron-electron interaction are given by the Coulomb integrals

$$V_{1234} = \int d\mathbf{r} \int d\mathbf{r}' \frac{\psi_1^*(\mathbf{r})\psi_2^*(\mathbf{r}')\psi_3(\mathbf{r})\psi_4(\mathbf{r}')}{|\mathbf{r} - \mathbf{r}'|} \tag{4}$$

where the ψ_n run over the eigenstates of the underlying one-electron hamiltonian. In standard LFM theory, ψ_n are the free ion $2p$ and $3d$ orbitals, while in quantum-chemistry configuration interaction methods, the $3d$ orbitals are replaced by molecular orbitals ψ_k. Here we project the valence eigenstates ψ_k onto the $3d$-orbitals such that $\psi_k = \sum_m C_{mk}\phi_m + \psi_L$, where ψ_L is the part of the wave function on the ligands. We first consider the case when there is exactly one molecular orbital ψ_k with symmetry m in the energy interval I. We then have $\psi_k \equiv \psi_m = \alpha_m \phi_m + \psi_L$. Putting this expression into Eq. (4) and neglecting all terms with one or more ψ_L, we get $V_{1234} \approx \alpha_1^*\alpha_2^*\alpha_3\alpha_4 V_{1234}^{at}$, where V_{1234}^{at} corresponds to the atomic orbitals ϕ_m. Following standard practice in multiplet theory, we obtain V^{at} from free ion integrals (V^{HF}) using Cowan's Hartree-Fock program and rescale them uniformly by a factor 0.9 in order to account for the neglect of (intra-atomic) configuration interaction in the Hartree-Fock approximation (Cowan, 1981). This results in the following working expression.

$$V_{1234} = \kappa_{1234} V_{1234}^{HF}, \quad \kappa_{1234} = 0.9\alpha_1^*\alpha_2^*\alpha_3\alpha_4 \tag{5}$$

We use Eq. (5) also for the general case when there is more than one molecular orbital per m and the covalency coefficients α_m are computed with Eq. (2). In standard LFM method, a single reduction factor κ is used. Here κ_{1234} is orbital dependent, since the covalency α_m depends on the $3d$ orbital symmetry m. This introduces an anisotropy of the Coulomb interaction matrix (5). We note that this effect is automatically included in quantum chemistry configuration interaction methods (Ogasawara et al., 2001; Ikeno et al., 2009), where the waves ψ_k entering Eq. (4) are molecular orbitals. To the best of our knowledge, however, the effect has not yet been considered in the framework of LFM theory. We shall see in the applications below that the α_m values typically vary in the range $0.75 \sim 0.95$ for the different d orbital symmetry m. The corresponding variation of Coulomb integral reduction factor κ is $0.3 \sim 0.8$ and so the anisotropy effect can be substantial. Core-valence Coulomb integrals are given by Eq. (4) with two core and two valence orbitals. We put $\alpha = 1$ for the core-orbitals, since they are not hybridized with the ligand states.

3. Results and discussion

We first apply the method to the transition metal monoxides MO (M = Mn,Fe,Co,Ni) in rocksalt structure. DFT calculations (Kresse and Furthmüller, 1996) were performed with the PBE exchange-correlation (XC) potential and experimental lattice constants. Fig. 1 shows the $3d$ partial DOS on the metal site for t_{2g}-symmetry (xy, yz, zx orbitals) and e_g-symmetry ($x^2 - y^2$, $3z^2 - r^2$ orbitals) in the non-magnetic state. Even though the true ground state of these metal oxides is antiferro-magnetic, we extract the ligand field parameters from the non-magnetic band structure, because ligand field splitting is essentially a one-electron, spin-independent effect due to electro-static field and orbital hybridization. Spin-polarization is taken account of in multiplet calculations through dd Coulomb interaction. Table 1 lists the ligand field parameters, calculated with an integration intervall $I = (-3,2)$ eV, covering the antibonding band. The $10Dq$ value of about 1 eV agrees well with empirical and ab initio values (de Groot et al., 1990; Ikeno et al., 2009). The covalency parameter α is systematically smaller for e_g than for t_{2g}, reflecting the stronger hybridization of the σ-bonds formed by the e_g-orbitals as compared to the π-bonds of t_{2g}. The anisotropic
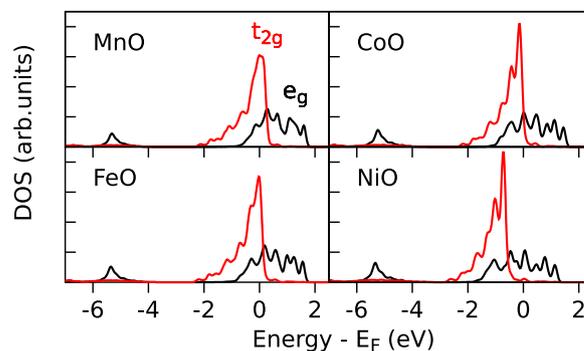
Fig. 1. Partial density of states (DOS) of transition metal monoxides projected on metal-$3d$ orbitals of t_{2g} (red) and e_g-symmetry (black).

Table 1
Calculated ligand field parameters of transition metal monoxides. $10Dq = E(t_{2g}) - E(e_g)$ in eV.

	MnO	FeO	CoO	NiO
$10Dq$	0.934	0.914	0.829	0.929
$\alpha(t_{2g})$	0.932	0.943	0.947	0.946
$\alpha(eg)$	0.906	0.907	0.903	0.891

effect is rather small but it increases when going from MnO to NiO, where $[\alpha(t_{2g})/\alpha(e_g)]^4 = 1.27$. This means that in NiO, the repulsion between two electrons occupying a t_{2g} orbital is larger by 27% than for two electrons occupying an e_g orbital.

Fig. 2 shows the L-edge spectra calculated in LFM theory with the ab initio ligand field parameters of Table 1. The threshold of the calculated spectra has been aligned with experiment. The line spectra were broadened with a lorentzian of width 0.3 and 0.5 eV in the L_3 and L_2 regions, respectively. The theoretical spectra agree very well with experiment. A few minor differences can be found. In the CoO spectrum, the peak intensity at 778 eV is slightly overestimated. In NiO, the weak hump at 867 eV is missing. This is likely a transition to continuum states, which cannot be captured in a single ion model (Krüger, 2010). Apart from these minor differences, the agreement between theory and experiment is excellent. It is as good as that obtained with quantum chemistry configuration interaction method by Ikeno et al. (2009). We now discuss the effect of the anisotropy of the Coulomb integral reduction in the case of NiO. In Fig. 1d, the blue spectrum ("iso") has been obtained by disreading the anisotropy, i.e. by applying a uniform Coulomb reduction factor $\kappa = 0.77$, obtained as the average of the calculated α_m^2 times 0.9. It can be seen that the "iso" spectrum lacks the small peak labeled 'A' and that the intensity ratio of the L_2 doublet (peak 'B') is somewhat less good than in the anisotropic calculation (red line). In the case of cubic transition metal monoxides the anisotropy effect is weak because of high symmetry and mainly ionic bonding. Nonetheless, including the anisotropic Coulomb reduction further improves the spectra as demonstrated here in the case of NiO.

As a second example, we apply our theory to nickel (NiPc) and cobalt phthalocyanine (CoPc) molecules. They have a flat geometry where the metal ion is bonded to four nitrogen ligands along the x- and y- axes of the molecular plane. The D_{4h} symmetry splits the $3d$-orbitals into four levels, a_{1g} ($3z^2 - r^2$), b_{1g} ($x^2 - y^2$), b_{2g} (xy) and e_g (xz, yz) (Bartolome, 2014). Fig. 3a,b shows the $3d$-DOS of the single molecules, calculated with VASP DFT-PBE in the theoretically optimized geometry. The antibonding, $3d$-like molecular orbitals are located above -3 eV. By direct inspection of the DOS, it can be seen that in both molecules the order of the ligand field splitting is $E(b_{2g}) < E(e_g) \approx E(a_{1g}) \ll E(b_{1g})$. Table 2 lists the calculated ligand field parameters obtained with the energy interval $I = (-3,4)$ eV. The anisotropy of the α values is very strong, with $\alpha(b_{1g})$ being much smaller than the other α_m. This reflects
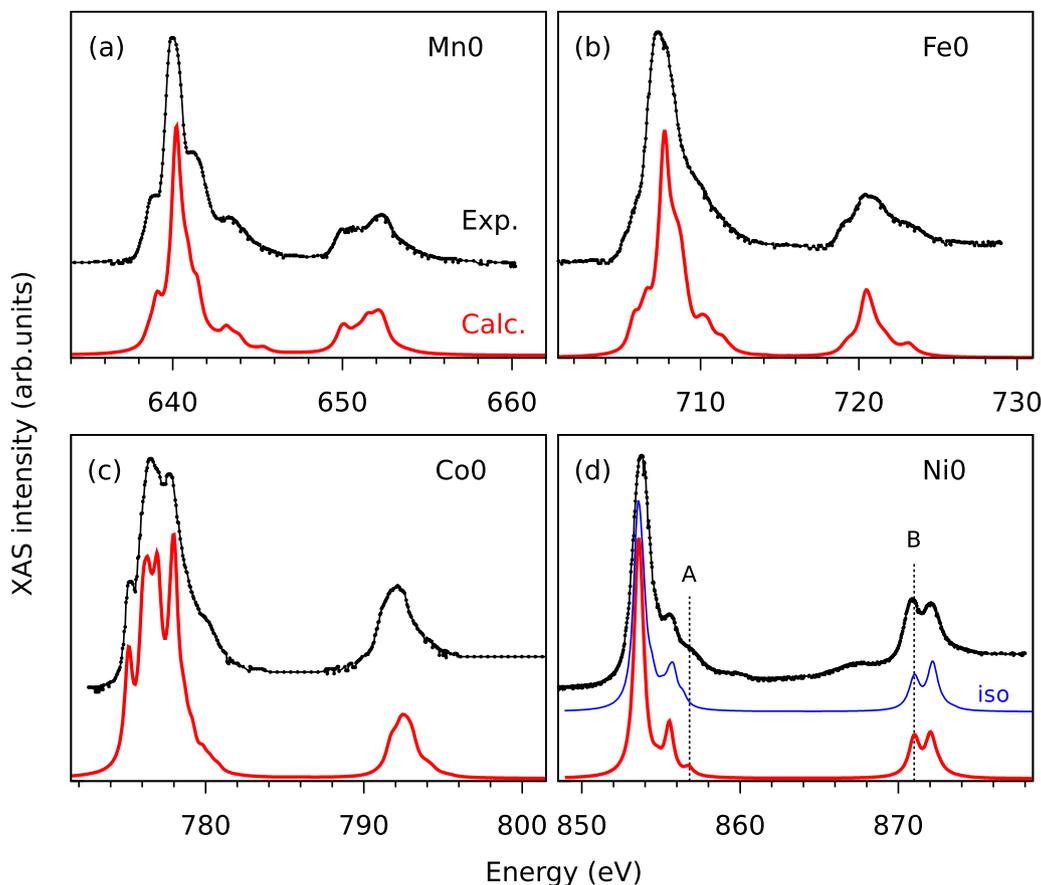
Fig. 2. X-ray absorption spectra of transition metal oxides. The thresholds of the calculated spectra (red) have been aligned with the experimental data (black), taken from Ikeno et al. (2009). In (d), the blue spectrum ("iso") corresponds to a standard calculation with orbital-independent Coulomb integral reduction.

the strong covalency of the $x^2 - y^2$ orbital, which forms σ-bonds with the four N ligands. In order to see the sensitivity of the results to the XC-potential, we have redone the NiPc and CoPc calculations in the LDA (not shown) while keeping the PBE-optimized molecular geometries. All ϵ_m and α_m values differ by less than 1% from PBE, i.e. the effect of the XC-potential on the obtained LFM parameters is negligible.

Both in DFT and in LFM model calculations we find that the ground state of NiPc is a (d^8) spin singlet with a ($a_{1g}^2 b_{2g}^2 e_g^4$) configuration in agreement with the literature (Bartolome, 2014). The calculated L-edge spectra are shown in Fig. 3c for linear polarization in-plane ($E\|xy$, black) and out-of-plane ($E\|z$, red). The NiPc in-plane spectrum shows essentially a single sharp line for L_3 and L_2, corresponding to transition from the $2p_{xy}$ orbitals to the 3d hole states of b_{1g} ($x^2 - y^2$) symmetry. The theoretical out-of-plane spectrum is virtually zero, because the dipole selection rules exclude $p \to d_{x^2-y^2}$ transitions for $E\|z$. In the experimental out-of-plane spectrum, some weak features are present. They may partly be attributed to metal-ligand back-bonding involving virtual molecular orbitals with a small contribution of Ni 3d and 4s orbitals of a_{1g} or e_g-symmetry, such as the tiny e_g peak seen in the DOS at 1 eV.

For CoPc, our spin-polarized DFT calculations (not shown) give a (d^7, $a_{1g}^1 b_{2g}^2 e_g^4$, $S = 1/2$) ground state, i.e. the third hole occupies the a_{1g} orbital. From the non-magnetic DOS in Fig. 3b, a hole in the a_{1g} or e_g orbital seems equally likely, but from the LFM calculation with the parameters of Table 2 we get a $^2A_{1g}$ ground state with dominant ($a_{1g}^1 b_{2g}^2 e_g^4$) occupation in agreement with the spin-polarized DFT result. The calculated spectrum obtained with the parameters in Table 2 is shown in Fig. 3g ("aniso", $^2A_{1g}$"). It agrees very well with the experimental data (Fig. 3h) taken from Kroll et al. (2009). The in-plane spectrum (black) is dominated by doublets around 782 eV (L_3) and 796 eV (L_2). They can be attributed to transitions into b_{1g} states split by

exchange coupling between the two final state 3d-holes. The out-of-plane L_3-spectrum shows a sharp peak at 799 eV which corresponds to the $2p_z \to 3d_{3z^2-r^2}$ transition. Here, no exchange splitting can occur, since both final 3d-holes are in the $3z^2 - r^2$-orbital and must form a singlet. The corresponding L_2 peak has much smaller intensity, both in theory and experiment. The experimental spectrum has another weak, but clearly visible peak at 782 eV (labeled 'A'), which is not reproduced in the calculation. We tentatively attribute this feature to a virtual molecular orbital of e_g symmetry, which gives rise to the small peak at 1.5 eV in the DOS (Fig. 3b) indicating some π-back donation from the N ligands.

Fig. 3f shows the spectrum obtained with an average, isotropic Coulomb reduction factor $\kappa = 0.75$. The ground state is still ($^2A_{1g}$) but the spectral shape is clearly changed and agrees less well with experiment. This proves that the anisotropy of the Coulomb reduction can have a substantial effect on the L-edge spectra and must in general not be neglected. As seen from Fig. 3b and Table 2, the e_g-a_{1g} level splitting is very small in CoPc. If the e_g level is lifted by 0.5 eV, the ground state switches to (^2E_g) with a ($a_{1g}^2 b_{2g}^2 e_g^3$) configuration. Fig. 3e shows the corresponding spectra, obtained with the α_m and ϵ_m values of Table 2, except for $\epsilon(e_g) = 0.408$ eV (or $10Dq = 3.09$, $Ds = 0.22$, $Dt = 0.34$.) While the overall spectral shape is rather similar to the ($^2A_{1g}$) ground state, there are a number of clear differences which considerably worsen the agreement with the data. An interesting feature is the absence of any L_2-peak in out-of-plane polarization. This can be understood as follows. For $E\|z$, we have the selectron rule $\Delta m_l = 0$, such that $p \to d_{x^2-y^2}$ transitions are impossible, as already in seen NiPc. As a consequence, the excited electron must fill the e_g hole, resulting in a ($a_{1g}^2 b_{2g}^2 e_g^4$) valence configuration which has $L = S = J = 0$. The L_2-edge ($2p_{1/2}$-hole) final state thus has a total angular momentum $J = 1/2$. Due to spin-orbit coupling, the ^2E_g ground state has an unquenched orbital moment
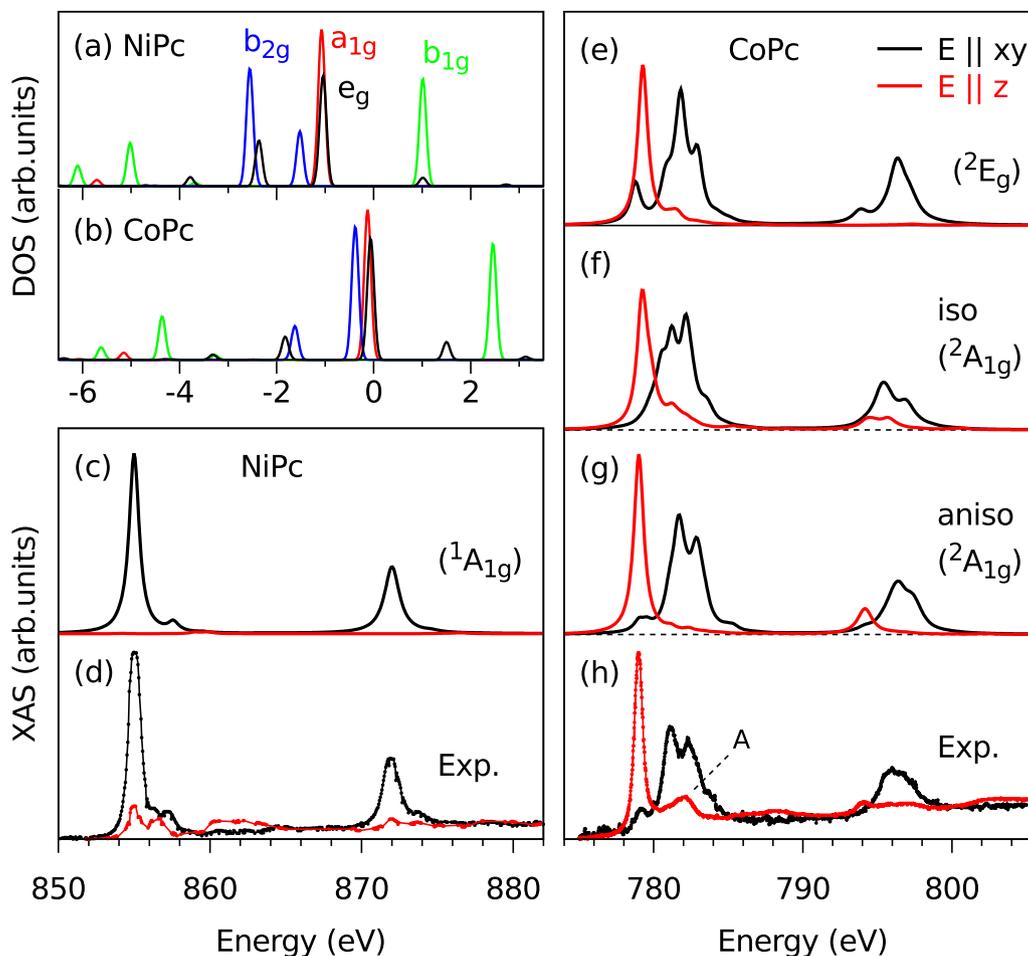
Fig. 3. Partial density of states (DOS) of NiPc (a) and CoPc (b) molecules ($E_F = 0$). (c, e-g) Calculated X-ray absorption spectra (XAS) for in-plane (black lines) and out-of-plane (red) polarization. (d, h) Experimental data Kroll et al., (2009, 2012).

Table 2
Calculated ligand field parameters of NiPc and CoPc. Energies in eV.

symmetry orbital	a_{1g} $3z^2 - r^2$	b_{1g} $x^2 - y^2$	b_{2g} xy	e_g xz, yz
NiPc				
ϵ_m	-1.084	1.003	-2.235	-1.252
α_m	0.918	0.759	0.961	0.946
	$10Dq = 3.24$, $Ds = 0.16$, $Dt = 0.29$			
CoPc				
ϵ_m	-0.135	2.450	-0.642	-0.092
α_m	0.906	0.796	0.955	0.949
	$10Dq = 3.09$, $Ds = 0.29$, $Dt = 0.28$			

$|M_L| = 1$ and a total moment $|M_J| = 3/2$. As $E\|z$ implies $\Delta M_J = 0$, the final state also has $|M_J| = 3/2$. This is impossible for the $2p_{1/2}$-hole with $J = 1/2$ which explains the absence of an out-of-plane L_2 peak.

From the X-ray spectra obtained with our non-empirical LFM method we thus conclude that the ground state of CoPc is $^2A_{1g}$ in agreement with our own spin-polarized DFT calculations and most of the experimental and theoretical literature (Bartolome, 2014; Kroll et al., 2009). Recently, Zhou et al. (2016) have calculated the L-edge spectra of CoPc in a charge transfer LFM model. They have stressed the importance of anisotropic covalency which is confirmed by our results (Figs. 3f,g). They further argued that the strong Co-N hybridization of the b_{1g} orbital cannot be modeled in a single-ion multiplet scheme and that charge transfer processes must explicitly be taken into account for satisfactory agreement with experiment. The present results do not support this conclusion. Indeed the single-ion LFM spectra of Fig. 3g

agree as well with experiment as the charge-transfer calculations in Ref. Zhou et al. (2016). Moreover, we have achieved this level of agreement without empirical parameters, while in Ref. Zhou et al. (2016) the ligand field and charge-transfer parameters have been fitted to experiment. We note that the single-ion LFM model used here, works best for ionic metal-ligand bonds. When the covalency increases, charge transfer effects become stronger and may need to be taken into account explicitly for an accurate description of the L-edge spectra.

4. Conclusions

In summary, we have developed a simple scheme for extracting ligand field model parameters from DFT calculations of solids or molecules. We have introduced an orbital-dependent Coulomb integral reduction factor, to take account of the anisotropy of the metal-ligand bonding. We have applied the method to transition metal monoxide solids, as well as nickel and cobalt phthalocyanine molecules and have obtained good agreement with experiment in all cases. In the case of phthalocyanine, the anisotropy of the covalency parameter is large and has a substantial effect on the spectra shape. For NiPc we find a $(a_{1g}^2 b_{2g}^2 e_g^4)$ singlet ground state and for CoPc a $(a_{1g}^1 b_{2g}^2 e_g^4)$ spin doublet, in agreement with the literature.

References

Bartolomé, J., Monton, C., Schuller, I.K., 2014. Magnetism of metal phthalocyanines. In: J. Bartolomé (Ed.), Molecular Magnets. Springer, Heidelberg.

Cowan, R.D., 1981. The Theory of Atomic Structure and Spectra. University of California Press, Berkeley.

de Groot, F., Kotani, A., 2008. Core Level Spectroscopy of Solids. CRC Press, Boca Raton.

de Groot, F.M.F., Fuggle, J.C., Thole, B.T., Sawatzky, G.A., 1990. 2p x-ray absorption of 3d transition-metal compounds: an atomic multiplet description including the crystal field. Phys. Rev. B 42, 5459–5468. https://doi.org/10.1103/PhysRevB.42.5459.

Ikeno, H., de Groot, F.M.F., Stavitski, E., Tanaka, I., 2009. Multiplet calculations of L2;3 xrayabsorption near-edge structures for 3d transition-metal compounds. J. Phys. Condens. Matter 21, 104208. https://doi.org/10.1088/0953-8984/21/10/104208. (17pp).

Krüger, P., 2010. Multichannel multiple scattering calculation of L2,3-edge spectra of TiO2 and SrTiO3: importance of multiplet coupling and band structure. Phys. Rev. B 81, 125121. https://doi.org/10.1103/PhysRevB.81.125121. (6pp).

Kresse, G., Furthmüller, J., 1996. Efficient iterative schemes for ab initio total-energy calculations using a plane-wave basis set. Phys. Rev. B 54, 11169–11186. https://doi.org/10.1103/PhysRevB.54.11169.

Kroll, T., Aristov, V.Yu., Molodtsova, O.V., Ossipyan, Yu.A., Vyalikh, D.V., Büchner, B., Knupfer, M., 2009. Spin and orbital ground state of Co in cobalt phthalocyanine. J. Phys. Chem. A 113, 8917–8922.

Kroll, T., Kraus, R., Schönfelder, R., Aristov, V.Yu., Molodtsova, O.V., Hoffmann, P., Knupfer, M., 2012. Transition metal phthalocyanines: insight into the electronic structure from soft x-ray spectroscopy. J. Chem. Phys. 137, 054306. https://doi.org/10.1063/1.4738754. (7pp).

Ogasawara, K., Iwata, T., Koyama, Y., Ishii, T., Tanaka, I., Adachi, H., 2001. Relativistic cluster calculation of ligand-field multiplet effects on $L_{2,3}$ cation x-ray-absorption edges of SrTiO$_3$, NiO, and CaF$_2$. Phys. Rev. B 64, 115413. https://doi.org/10.1103/PhysRevB.64.115413.

Thole, B.T., van der Laan, G., 1988. Branching ratio in x-ray absorption spectroscopy. Phys. Rev. B 38, 3158–3171. https://doi.org/10.1103/PhysRevB.38.3158.

van der Laan, G., Thole, B.T., Sawatzky, G.A., Verdaguer, M., 1988. Multiplet structure in the $L_{2,3}$ x-ray-absorption spectra: a fingerprint for high- and low-spin Ni^{2+} compounds. Phys. Rev. B 37, 6587–6589. https://doi.org/10.1103/PhysRevB.37.6587.

Yamaguchi, T., Shibuya, S., Suga, S., Shin, S., 1982. Inner-core excitation spectra of transition-metal compounds: ii. p-d absorption spectra. J. Phys. C 15, 2641–2650.

Zhou, J., Zhang, L., Hu, Z., Kuo, C., Liu, H., Lin, X., Wang, Y., Pi, T.-W., Wang, J., Zhang, S., 2016. The significant role of covalency in determining the ground state of cobalt phthalocyanines molecule. AIP Adv. 6, 035306. https://doi.org/10.1063/1.4943773.